

**POTENTIAL USE OF NANOCCLAY IN
DYE-SENSITIZED SOLAR CELL WITH NATURAL DYE**



Ni-on Saelim

A Dissertation Submitted in Partial Fulfilment of the Requirements
for the Degree of Doctor of Philosophy
The Petroleum and Petrochemical College, Chulalongkorn University
in Academic Partnership with
The University of Michigan, The University of Oklahoma,
and Case Western Reserve University

2012

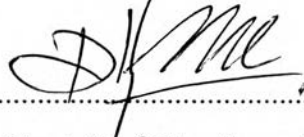
551743

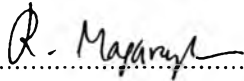
Thesis Title: Potential Use of Nanoclay in Dye Sensitized Solar Cell with Natural Dye
By: Ni-on Saelim
Program: Petrochemical Technology
Thesis Advisors: Assoc. Prof. Rathanawan Magaraphan

Accepted by The Petroleum and Petrochemical College, Chulalongkorn University, in partial fulfilment of the requirements for the Degree of Doctor of Philosophy.

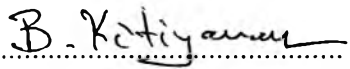

..... College Dean
(Asst. Prof. Pomthong Malakul)

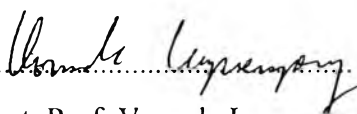
Thesis Committee:


.....
(Asst. Prof. Pomthong Malakul)


.....
(Assoc. Prof. Rathanawan Magaraphan)


.....
(Prof. Sumaeth Chavadej)


.....
(Asst. Prof. Boonyarach Kitiyanan)


.....
(Asst. Prof. Vorrada Loryuenyong)

ABSTRACT

5081001063: Petrochemical Technology Program

Ni-on Saelim: Potential Use of Nanoclay in Dye Sensitized Solar Cell with Natural Dye

Thesis Advisor: Assoc. Prof. Ratanawan Magaraphan 190 pp.

Keywords: Titanium dioxide/ Clay/ Na-bentonite/ Natural dye/ Electrophoretic deposition/ Gel electrolyte

The incorporation of clay in photoelectrode and electrolyte of dye-sensitized solar cell (DSSC) was scrutinized. Extracted red cabbage was found to be the best efficient natural dye in this study. The novel additives for natural dye, i.e. 4-chloro-2,5-difluorobenzoic acid and 4-(chloromethyl)benzoyl chloride alter the photovoltaic properties of DSSCs with the unchanged of overall conversion efficiency. The electrodes were prepared from both P25 TiO₂/bentonite and sol-gel TiO₂/bentonite composites with two kind of bentonite, CTAB-modified bentonite and purified Na-bentonite. The CTAB modified bentonite is better to be incorporated with P25 while purified Na-bentonite reduces crack formation of thick sol-gel TiO₂ and improve cell efficiency when its composite was applied on the top of transparent sol-gel TiO₂ as a scattering layer. To contribute the energy barrier function of bentonite, the electrophoretic deposition (EPD) was selected besides doctor blading to improve the electronic contact between TiO₂ and non-modified bentonite. However, it is too thick of stack bentonites that inhibit the function. Moreover, gel electrolyte prepared by the incorporation of clay particles in liquid electrolyte was studied. The CTAB Na-bentonite was compared to synthetic laponite in terms of photovoltaic properties and stability. Meanwhile, Na-bentonite, inability to solidify electrolyte itself was applied to an aerogel, the support of polymethyl acrylate since clay acts as a solid part, and polymer acts as a liquid cage. The optimal clay and polymer content was determined to obtain the good gel that provides a good DSSC efficiency along with ease of DSSC fabrication.

บทคัดย่อ

นอร์ แซ่ลิม : ชื่อหัวข้อวิทยานิพนธ์ (ภาษาไทย) การประยุกต์ใช้แร่ดินเหนียวในเซลล์แสงอาทิตย์ชนิดสีย้อมไวแสงกับสีย้อมธรรมชาติ (ภาษาอังกฤษ)(Potential Use of Nanoclay in Dye-Sensitized Solar Cell with Natural Dye) อาจารย์ที่ปรึกษา: รศ.ดร. รัตนาวรรณ มกรพันธุ์ 190 หน้า

แร่ดินเหนียวถูกนำมาประยุกต์ใช้ในแสงอาทิตย์ชนิดสีย้อมไวแสงโดยเติมลงในส่วนที่เป็นสารกึ่งตัวนำขั้วลบและในของเหลวอิเล็กโทรไลต์และใช้สีย้อมจากธรรมชาติเป็นตัวให้อิเล็กตรอนกับเซลล์ ในบรรดาสีธรรมชาติที่ศึกษาในงานวิจัยนี้พบว่าสีย้อมจากกระหล่ำม่วงให้ประสิทธิภาพสูงสุด ขณะเดียวกันสารตัวเติมใหม่ในการทดลองนี้ของสีย้อมจำพวกเบนโซอิก แอซิด และ เบนโซอิกคลอไรด์ ที่ใช้เป็นตัวดูดซับร่วมกับสีย้อม ให้ผลของสมบัติทางแสงเปลี่ยนเป็นไฟฟ้าที่ต่างกัน แต่ยังคงให้ประสิทธิภาพรวมไม่ต่างกันและไม่ต่างจากเซลล์ที่ไม่ใส่สารตัวเติมอิเล็กโทรดที่ใช้นั้นเตรียมได้จากทั้งคอมโพสิตของทีเทเนียมไดออกไซด์ P-25 และจากโซล-เจลทีเทเนียมไดออกไซด์ผสมกับแร่ดินเหนียวสองชนิดคือ เบนโทไนด์ชนิดดัดแปลงอินทรีย์ชนิดซีเท็ปและโซเดียมเบนโทไนด์ เบนโทไนด์ชนิดดัดแปลงอินทรีย์ชนิดซีเท็ปสามารถรวมตัวกับ P-25 ได้ดีกว่า ขณะที่โซเดียมเบนโทไนด์ลดการเกิดรอยแตกของชั้นโซล-เจลทีเทเนียมไดออกไซด์ที่หนาและเพิ่มประสิทธิภาพเซลล์เมื่อเมื่อคอมโพสิตเคลือบอยู่บนชั้นโซล-เจลทีเทเนียมไดออกไซด์ที่โปร่งใสโดยทำหน้าที่เป็นชั้นกระจ่าง เพื่อให้มีส่วนในการทำหน้าที่เป็นระดับพลังงานกันของเบนโทไนด์ เทคนิคการเตรียมฟิล์มด้วยวิธีทางไฟฟ้า ได้นำมาใช้นอกเหนือจากวิธีการปาดแบบคอกเตอร์ ซึ่งคาดว่าจะช่วยเพิ่มการสัมผัสระหว่างพื้นผิวและอนุภาคระหว่างเจลทีเทเนียมไดออกไซด์และโซเดียมเบนโทไนด์แต่ชั้นเบนโทไนด์ที่หนาเกินไปทำให้ไม่สามารถทำหน้าที่ดังกล่าวได้ นอกจากนี้ยังได้ศึกษาการเตรียมเจลอิเล็กโทรไลต์ที่ได้จากการผสมกันระหว่างแร่ดินเหนียวและของเหลวอิเล็กโทรไลต์ โดยที่เบนโทไนด์ชนิดดัดแปลงอินทรีย์ชนิดซีเท็ปนำมาเปรียบเทียบกับแร่ดินเหนียวสังเคราะห์ลาโปไนต์ในเทอมของสมบัติทางแสงไฟฟ้าและความเสถียรของเซลล์ ขณะที่โซเดียมเบนโทไนด์ที่ไม่สามารถทำให้เกิดเจลอิเล็กโทรไลต์ได้ก็ถูกนำมาทำให้มีโครงสร้างแบบแอโรเจลและเป็นที่ยึดอยู่ของพอลิเมทริลอะคริเลต โดยที่เบนโทไนด์จะทำหน้าที่เป็นของแข็งและพอลิเมอร์ช่วยกักเก็บของเหลวไว้ภายในคอมโพสิต ทั้งนี้สัดส่วนของแร่ดินเหนียวและพอลิเมอร์และสัดส่วนของคอมโพสิตที่เหมาะสมจะช่วยให้ได้เจลที่ให้ประสิทธิภาพของเซลล์ดีและง่ายต่อการประกอบเซลล์

ACKNOWLEDGEMENTS

First the author gratefully acknowledges Assoc. Prof. Rathanawan Magaraphan, my advisor from The Petroleum and Petrochemical College, Chulalongkorn University for providing valuable guidance, inspiration, encouragement, and opportunities. Also, my gratefully acknowledgement is given to Asst. Prof. Thammanoon Srithawong for his advice, encouragement, and assistance.

I would like to express my appreciation to Prof. Michael Grätzel, and his research associates, Dr. Shaik Mohammad Zakeeruddin, and Dr. Paul Liska from Laboratory of Photonics and Interfaces, Swiss Federal Institute of Technology in Lausanne (EPFL) for their contribution, advices, and opportunities that gave me worth experiences in the DSSC research field.

I would like to appreciate all faculty members and staffs at The Petroleum and Petrochemical College, Chulalongkorn University for their knowledge and assistance, especially Prof. Suwabun Chirachanchai and Prof. Anuvat Sirivat for the kind support of a potentiostat and a rheometer, respectively. In addition, my appreciation is given to Asst. Prof. Sojipong Chattraporn from the department of Physics, Chulalongkorn University for the kind support of I-V measuring instrument.

Moreover, I would like to give my special thanks to all members in my research group both from the Petroleum and Petrochemical College, Chulalongkorn University and from Laboratory of Photonics and Interfaces, Swiss Federal Institute of Technology in Lausanne (EPFL), as well as all of my friends for their friendship, encouragement, and kind assistance.

I am grateful for the financial support provided by the Thailand Research Fund through the Royal Golden Jubilee Ph.D. Program; Polymer Processing and Polymer Nanomaterials Unit, the Rachadapisek Sompoch Endowment; National Nanotechnology Center, National Science and Technology Development Agency, Thailand; the Petroleum and Petrochemical College; and the Center of Excellence on Petrochemical and Materials Technology, Thailand.

Finally, I wish to express my deep gratitude to my family for their love, understanding and encouragement during all these years spent for my Ph.D. study.

TABLE OF CONTENTS

	PAGE
Title Page	i
Abstract (in English)	iii
Abstract (in Thai)	iv
Acknowledgements	v
Table of Contents	vi
List of Tables	x
List of Figures	xii
Abbreviations	xvii
List of Symbols	xx
CHAPTER	
I INTRODUCTION	1
II LITERATURE REVIEW	3
III EXPERIMENTAL	58
IV PREPARATION AND APPLICATION OF TITANIUMDIOXIDE/MODIFIED NATURAL CLAY SEMICONDUCTOR AS A POTENTIAL ELECTRODE FOR NATURAL DYE-SENSITIZED SOLAR CELL	64
4.1 Abstract	64
4.2 Introduction	64
4.3 Experimental	66
4.4 Results and Discussion	68
4.5 Conclusions	71

CHAPTER	PAGE
4.6 Acknowledgements	71
4.7 References	72
V FABRICATION OF TITANIUMDIOXIDE/PURIFIED SODIUM- BENTONITE AND TITANIUM/CTAB- MODIFIED SODIUM-BENTONITE COMPOSITES FOR DSSC ELECTRODES	79
5.1 Abstract	79
5.2 Introduction	79
5.3 Experimental	81
5.4 Results and Discussion	84
5.5 Conclusions	87
5.6 Acknowledgements	88
5.7 References	88
VI PREPARATION OF SOL-GEL/PURIFIED SODIUM-BENTONITE COMPOSITES AND THEIR PHOTOVOLTAIC APPICATION FOR DYE-SENSITIZED SOLAR CELLS	96
6.1 Abstract	96
6.2 Introduction	96
6.3 Experimental	97
6.4 Results and Discussion	99
6.5 Conclusions	101
6.6 Acknowledgements	101
6.7 References	101

CHAPTER		PAGE
VII	ELECTROPHORETIC DEPOSITION OF TITANIUMDIOXIDE/PURIFIED SODIUM- BENTONITE COMPOSITES FOR DSSC ELECTRODES	108
	7.1 Abstract	108
	7.2 Introduction	108
	7.3 Experimental	110
	7.4 Results and Discussion	113
	7.5 Conclusions	116
	7.6 Acknowledgements	117
	7.7 References	117
VIII	ELECTROPHORETIC DEPOSITION OF TITANIUMDIOXIDE/PURIFIED SODIUM- BENTONITE COMPOSITES FOR DSSC ELECTRODES	129
	8.1 Abstract	129
	8.2 Introduction	129
	8.3 Experimental	131
	8.4 Results and Discussion	132
	8.5 Conclusions	135
	8.6 Acknowledgements	135
	8.7 References	136
IX	GEL ELECTROLYTE OF POLYMETHYL ARCYLATE AND CLAY AEROGEL FOR DYE-SENSITIZED SOLAR CELLS	143
	9.1 Abstract	143
	9.2 Introduction	143

CHAPTER	PAGE
9.3 Experimental	144
9.4 Results and Discussion	147
9.5 Conclusions	150
9.6 Acknowledgements	150
9.7 References	150
X CONCLUSIONS AND RECOMMENDATIONS	158
REFERENCES	161
APPENDICES	179
Appendix A Calculations of Ti:Si Molar Ratio	179
Appendix B Supplementary Results of Chapter IV	182
Appendix C Supplementary Results of Chapter V	183
Appendix D Supplementary Results of Chapter VI	185
Appendix E Supplementary Results of Chapter VII	188
CURRICULUM VITAE	189

LIST OF TABLES

TABLE		PAGE
CHAPTER II		
2.1	Spectral data and photovoltaic efficiency of rutinium-based dyes with acetonitrile-based electrolyte	18
2.2	Spectral data and photovoltaic efficiency of organic dyes with ionic liquid electrolyte	24
2.3	Classification of phyllosilicates according to the localization and abundance of crystalline lattice substitutions	49
CHAPTER III		
3.1	Main compositions of bentonite	61
CHAPTER IV		
4.1	Effect of natural dye sensitizers on photovoltaic properties of DSSCs fabricated with different photoanodes	75
4.2	Effect of additives on photovoltaic properties of DSSCs fabricated with TiO ₂ /clay electrode and sensitized with red cabbage dye	75
CHAPTER V		
5.1	Specific surface area results of the semiconductors fabricated with P25 TiO ₂ pastes containing different bentonite contents	92
5.2	Photovoltaic properties of DSSCs sensitized by red cabbage dye with photoanode thickness of about 6 μm at 500°C	93

TABLE		PAGE
CHAPTER VI		
6.1	Textural properties of the semiconductor electrodes obtained from N ₂ adsorption-desorption analysis	104
6.2	Photovoltaic properties of DSSCs sensitized by red cabbage dye	104
6.3	Photovoltaic properties of DSSCs fabricated with light scattering layer and sensitized by red cabbage dye	105
CHAPTER VII		
7.1	Effect of natural dye sensitizers on photovoltaic properties of DSSCs fabricated with different photoanodes	123
CHAPTER VIII		
8.1	Photovoltaic properties of DSSCs with various CB contents in Z646 electrolyte	138
8.2	Comparison of cell performance between DSSC with CB and DSSC with L-RD at full-sun light intensity	138
8.3	Stability testing of DSSCs with Z655 gel electrolyte compared to standard cell	139

LIST OF FIGURES

FIGURE	PAGE
CHAPTER II	
2.1	Band structures of differently-doped semiconductors. 3
2.2	Principle of photovoltaic device. 4
2.3	The current-voltage (black) and power-voltage (gray) characteristics of an ideal cell. Power density reaches a maximum at a bias V_m , close to V_{oc} . The maximum power density $J_m \times V_m$ is given by the area of the inner rectangle. The outer rectangle has area $J_{sc} \times V_{oc}$. 5
2.4	Effect of (a) increasing series and (b) reducing parallel resistances. In each case, the outer curve has $R_s = 0$ and $R_{sh} = \infty$. In each case, the effect of the resistances is to reduce the area of the maximum power rectangle compared to $J_{sc} \times V_{oc}$. 7
2.5	Photocurrent action spectra of TiO_2 electrodes (12 μm P25) sensitized with different Ru(II) bipyridine complexes, electrolyte: 80% ethylene carbonate, 20% propylene carbonate, 0.5 M KI, 40 mM I_2 , a) bare TiO_2 electrode, b) RuL_3 ($L = 2,2'$ -bipyridine-4,4'-dicarboxylate) adsorbed from water, pH 4.8, c) $RuL_2(NSC)_2$ and d) $RuL_2[Ru(bpy)_2(CN)_2]_2$ adsorbed from ethanol. 9
2.6	Principle of operation of dye-sensitized solar cell. 11
2.7	Energy-level diagram of a dye-sensitized nanocrystalline semiconductor solar cell. 12
2.8	The relative energies of the π molecular orbitals of ethane and 1,3-butadiene. 15
2.9	Molecular structure of ruthenium (II) dyes N3, N719 and Black dye, and IPCE spectra of N3 and black dye. 17

FIGURE	PAGE
2.10 Molecular structure of heteroleptic ruthinium-based dyes.	20
2.11 The molecular structure of organic dyes.	22
2.12 Schematics of (a) anthocyanin structure, and (b) the binding between anthocyanin and TiO ₂ particles.	25
2.13 Betalain pigments.	26
2.14 Carotenoid structures.	26
2.15 The chemical structure of chlorophyll a.	28
2.16 The chemical structure of Cu-2- α -oxymesoisochorin e ₄ .	28
2.17 The chemical structures of cholic acid and its derivatives.	28
2.18 Schematics of a) dehydroxylated TiO ₂ surface and b) chemisorption of carboxyl group of dye on TiO ₂ surface.	31
2.19 Scheme showing the important kinetic parameters with surface states.	32
2.20 The molecular structure of additives in electrolyte.	36
2.21 The chemical structure of spiro-OMeTAD.	39
2.22 The chemical structure of P(VP-co-AN).	41
2.23 The chemical structures of co-adsorbates.	43
2.24 Montmorillonite structure.	48
2.25 Powder X-ray diffraction pattern for (a) montmorillonite, (b) pillared montmorillonite, and (c) iron-doped pillared montmorillonite.	50
2.26 a) pillared clay, b) organoclay, and c) porous clay heterostructure.	50
2.27 (A) stable gel, (B) nucleation at the edge of the vial, (C) ice growth toward the center of vial, (D) frozen solution, (E) after sublimation.	52
2.28 FE-SEM micrograph of the clay aerogel.	53
2.29 Schematic of cathodic electrophoretic deposition (EPD) and electrolytic deposition (ELD).	55

FIGURE	PAGE
CHAPTER III	
3.1 The photoanode film.	62
3.2 DSSC configuration.	62
CHAPTER IV	
4.1 UV-visible absorption spectra of (a) red cabbage, (b) rosella, and (c) blue pea: (---) adsorbed on TiO ₂ /clay electrode, (.....) adsorbed on pure TiO ₂ electrode, and (—) in as-prepared solution.	76
4.2 XRD patterns of (a) TiO ₂ /modified natural clay and (b) pure TiO ₂ electrodes.	77
4.3 Top-viewed SEM micrograph (a), corresponding EDX Si mapping (b), and high-resolution cross-sectional SEM micrograph (c) of TiO ₂ /modified natural clay electrode.	78
CHAPTER V	
5.1 Top-viewed FE-SEM micrographs of (a) P25 TiO ₂ electrode, (b) P25 TiO ₂ /5 mol% Si purified Na-bentonite electrode, (c) P25 TiO ₂ /5 mol% Si CTAB-modified Na-bentonite electrode, and cross-sectional FE-SEM micrographs of (d) P25 TiO ₂ /bentonite.	94
5.2 Optical microscopy images of (a) P25 TiO ₂ electrode, (b) P25 TiO ₂ /purified Na-bentonite electrode, and (c) P25 TiO ₂ /CTAB-modified Na-bentonite electrode.	95

FIGURE	PAGE
CHAPTER VI	
6.1 XRD patterns of (a) sol-gel TiO ₂ , (b) sol-gel TiO ₂ /5 mol% Si purified Na-bentonite, (c) sol-gel TiO ₂ /10 mol% Si purified Na-bentonite electrodes and (d) purified Na-bentonite.	106
6.2 SEM micrograph (a) and TEM micrograph (b) of sol-gel TiO ₂ .	106
6.3 Cross-sectional SEM micrographs of (a) sol-gel TiO ₂ and (b) sol-gel TiO ₂ /5 mol% Si purified Na-bentonite electrodes.	107
CHAPTER VII	
7.1 The cross-sectional-viewed FE-SEM micrographs of composite film.	124
7.2 Top-viewed FE-SEM micrographs of (a) 0-ben, (b) 5-ben, (c) 10-ben, (d) 20-ben, and magnified micrograph of (e) 0-ben and (f) 20-ben.	125
7.3 Top-viewed FE-SEM micrographs of (a) 4 μm at 4th layer, (b) 5.5 μm at 5th layer, and (c) 12.5 μm at 12th layer.	126
7.4 The spectra of red cabbage dye adsorbed on deposited films with the subtraction of deposited films and glass substrates.	127
7.5 The photovoltaic properties, (a) short circuit current, J _{sc} , (b) open circuit voltage, V _{oc} , (c) fill factor, FF, and (d) conversion efficiency, η% of DSSC with TiO ₂ /clay composite electrodes at various clay contents and film thicknesses.	128

FIGURE	PAGE
CHAPTER VIII	
8.1 The optical properties of gel electrolyte containing CB and L-RD.	140
8.2 J-V curves for the DSSCs with Z646 liquid and its gel electrolytes.	141
8.3 J-V curves for the DSSCs with Z655 liquid its gel electrolytes with various CB contents.	141
8.4 Stability test of standard cell and cells with gel electrolyte at 60°C under 1.5 AM sun simulator.	142
CHAPTER IX	
9.1 Nyquist diagram of the impedance spectra of PMA90 at amplitude of 0.3 V (a) and equivalent electrical circuit model of symmetric cell (Pt//gel electrolyte//Pt), R_s is ohmic series resistance, R_p is charge transfer resistance ($p = ct$), R_d is diffusion resistance, and CPE is constant phase element (b).	153
9.2 The FE-SEM micrograph of PMA beads.	154
9.3 The FE-SEM micrograph of PMA/purified Na-bentonite aerogel.	154
9.4 The FE-SEM micrograph of PMA film coating on clay aerogel.	155
9.5 Figure 9.5 Dynamic frequency sweep data of (a) PMA100, (b) PMA90, (c) PMA75 at various contents in liquid electrolyte.	156
9.6 Diffusion conductivity of gel electrolytes at various solid content in liquid electrolyte.	157

ABBREVIATIONS

Al ₂ O ₃	Aluminium oxide
AMII	1-Allyl-3-methylimidazolium iodide
BAU	Business as usual
BMII	1-Butyl-3-methylimidazolium iodide
Br ⁻	Bromide
Br ₂	Bromine
CaCO ₃	Calcium carbonate
CdS	Cadmium sulfide
CdSe	Cadmium selenide
CTAB	Cetyltrimethylammoniumbromide
CuI	Copper iodide
CuSCN	Copper thiocyanate
DMF	N,N-dimethylformamide
DMII	Dimethylimidazoliumiodide
DMSO	Dimethylsulfoxide
D-π-A	Electron donor-conjugate spacer-electron acceptor
DPA	1-Decylphosphonic acid
DSSC	Dye-sensitized solar cell
DSC	Dye-sensitized solar cell
DYSC	Dye-sensitized solar cell
ELD	Electrolytic deposition
EMIDCN	1-Methyl-3-ethylimidazolium dicyanamides
EMII	1-Ethyl-3-methylimidazolium iodide
EMINCS	1-Ethyl-3-methylimidazolium thiocyanate
EMITCM	1-Ethyl-3-methylimidazolium tricyanomethanide
EMITCB	1-Ethyl-3-methylimidazolium tetracyanoborate
EPD	Electrophoretic deposition
FF	Fill factor
FTO	Fluorine-doped tin oxide
GBA	4-guanidinobutyric acid

GuNCS	Guanidine thiocyanate
HCl	Hydrochloric acid
HDMA	Hexadecylmalonic acid
HOMO	Highest occupied molecular orbital
HMII	1-Hexyl-3-methylimidazolium iodide
HTM	Hole transport material
I ⁻	Iodide
I ₂	Iodine
I ₃ ⁻	Triiodide
IL	Ionic liquid
IPCE	Incident photon to current conversion efficiency
KI	Potassium iodide
LHE	Light harvesting efficiency
LiI	Lithium iodide
LMCT	Ligand to metal charge transfer
LUMO	Lowest unoccupied molecular orbital
MgO	Magnesium oxide
MLCT	Metal to ligand charge transfer
MO	Molecular orbital
MMT	Montmorillonite
MPN	3-Methoxypropionitrile
Nb ₂ O ₅	Niobium pentoxide
NBB	N-butylbenzimidazole
NCS	Thiocyanate group
NHE	Normal hydrogen electrode
NMBI	N-methyl benzimidazole
NMB	N-methyl benzimidazole
NMP	N-methyl-2-pyrrolidone
PAA	Polyacrylic acid
PAM	Polyacrylamide
PAN	Polyacrylonitrile
PEO	Polyethylene oxide

PMMA	Polymethyl methacrylate
PMII	1-Propyl-3-methylimidazolium iodide
PNIPAAm	Poly (n-isopropylacrylamide)
PPA	3-Phenylpropionic acid
PV	Photovoltaic
PVDF-HFP	Polyvinylidene fluoride-co-hexafluoropropylene
PVP	Polyvinylpyridine
P(VP-co-AN)	Poly(vinylpyridine-co-acrylonitrile)
RTIL	Room temperature ionic liquid
Ru	Rutinium
SCN ⁻	Thiocyanate
(SCN) ₂	Thiocyanogen
SeCN ⁻	Selenium cyanate
(SeCN) ₂	Selenium cyanogen
SiO ₂	Silica oxide
SnO ₂	Tin oxide
SrO	Strontium oxide
STC	Standard Test Condition
SrTiO ₃	Strontium titanate
Ta ₂ O ₅	Tantalum pentoxide
TBP	4-tert-butylpyridine
TCO	Transparent conductive oxide
THF	Tetrahydrofuran
TiCl ₄	Titanium tetrachloride
TiO ₂	Titanium dioxide
UV	Ultraviolet
Vis	Visible
WEO	World Energy Outlook
WO ₃	Tungsten oxide
ZnO	Zinc oxide
ZrO ₂	Zirconium oxide

LIST OF SYMBOLS

E_{cb}	conduction-band edge
E_{redox}	redox electrolyte energy
E_f	Fermi level
C_{ss}	surface state capacity
C_H	Helmholtz layer capacity
J	Photo densities
J_m	Maximum-current point
J_{sc}	Shot circuit current
V	Voltage
V_{oc}	Open circuit voltage
V_m	Maximum-voltage point
P	Power density
η	Conversion efficiency
R_s	Series resistance
R_{sh}	Shunt resistance
e	Electron
Φ_{inj}	Quantum yield of charge injection
η_c	Efficiency of collecting the injected charge at the back contact
ϵ_{max}	Molar extinction coefficient